Structural Engineering and Mechanics, Vol. 12, No. 1 (2001) 101-118
DOI: http://dx.doi.org/10.12989/sem.2001.12.1.101

Hydroelastic vibration analysis of wetted thin-walled structures by coupled FE-BE-Procedure

Udo Röhr† and Peter Möller‡

Department of Mechanical Engineering, University of Rostock, Albert-Einstein-Str. 2, 18059 Rostock, Germany

Abstract. The reliable prediction of elastic vibrations of wetted complex structures, as ships, tanks, offshore structures, propulsion components etc. represent a theoretical and numerical demanding task due to fluid-structure interaction. The paper presented is addressed to the vibration analysis by a combined FE-BE-procedure based on the added mass concept utilizing a direct boundary integral formulation of the potential fluid problem in interior and exterior domains. The discretization is realized by boundary element collocation method using conventional as well as infinite boundary element formulation with analytical integration scheme. Particular attention is devoted to modelling of interior problems with both several separate or communicating fluid domains as well as thin-walled structures wetted on both sides. To deal with this specific kind of interaction problems so-called "virtual" boundary elements in areas of cut outs are placed to satisfy the kinematical conditions in partial connected fluid domains existing in realistic tank systems. Numerical results of various theoretical and practical examples demonstrate the performance of the BE-methodology presented.

Key words: fluid structure interaction; vibration analysis; coupled finite and boundary element method; potential problem.

1. Introduction

Prognoses of global and local vibration characteristics of ship structures are essential in modern product development. The growing tendency towards three-dimensional finite-element models requires physically adequate fluid modelling for the hydroelastic vibration problem.

The discrete equations of motion for the linear elastic structure are formulated in the known way, (1).

$$\boldsymbol{M} \cdot \ddot{\boldsymbol{D}} + \boldsymbol{B} \cdot \dot{\boldsymbol{D}} + \boldsymbol{K} \cdot \boldsymbol{D} = \boldsymbol{F} + \boldsymbol{F}_{\boldsymbol{H}} \tag{1}$$

$\boldsymbol{M}$, $\boldsymbol{B}$ and $\boldsymbol{K}$ represent the inertial, damping and stiffness features of the structure as consistent matrices; $\ddot{\boldsymbol{D}}$, $\dot{\boldsymbol{D}}$ and $\boldsymbol{D}$ are the discrete acceleration, velocity and displacement vectors. Outer excitation forces $\boldsymbol{F}$ as well as the force vector $\boldsymbol{F}_{\boldsymbol{H}}$ are parts of (1). $\boldsymbol{F}_{\boldsymbol{H}}$ represents the interaction between elastic-kinetic behaviour of the structure and the surrounding fluid, caused by the hydrodynamic pressure distribution p on the wetted surface. In case of linear ship structure vibration that are hydrodynamic inertial effects.

† Professor
‡ Senior Research Scientist

Especially at higher frequencies a spatial interactive flow pattern exists near the ship hull due to the complex structure deformation. After usual physical simplifications this interaction is described by the proportionality (2) with the hydrodynamic added mass matrix $\boldsymbol{M_H}$.

$$\boldsymbol{F_H} = -\boldsymbol{M_H} \cdot \ddot{\boldsymbol{D}} \tag{2}$$

Starting point to evaluate the global vibration behaviour is the knowledge of the natural spectrum, the solution of the general eigenvalue problem (3).

$$[\boldsymbol{K} - \omega^2(\boldsymbol{M} + \boldsymbol{M_H})] \cdot \boldsymbol{D} = 0 \tag{3}$$

Early complex investigations (Camisetti 1979, Geßner and Schmitz 1983, Payer 1981, Skaar and Carlsen 1979) on (3) done by finite element method were simplifying the three-dimensional interaction problem and dealing with the two-dimensional rigid body flow problem in form of the well-known added masses by Lewis (Lewis 1929, Landweber 1957). This procedure is widely used in practice since it is simple (diagonal added mass matrix), despite known physical restrictions (Payer and Asmussen 1985, Payer and Pleß 1985).

On the other hand the three-dimensional hydrodynamic mass effect in case of ship structure vibrations has been demonstrated by more detailed calculation models since the early eighties. Additional effects caused by shallow water can be taken into account in this way only.

The aim of this paper is to present an effective boundary element method to take the hydrodynamic inertial effects into consideration. Some principal cases of application are shown in Fig. 1.

2. The mathematical model

Calculation models combining finite element and boundary element method (FEM-BEM) prove their suitability in many technical applications dealing with structure problems in contact with an unbounded continuum. Linear structure vibrations are in general considered as boundary value problem for the velocity potential in a three-dimensional fluid which is incompressible and free of rotation and friction (Armand and Orsero 1979). Vibration induced waves on the free surface are of low influence on the flow pattern near the motionless ship (Hakala 1986) and can be neglected. Damping is not considered.

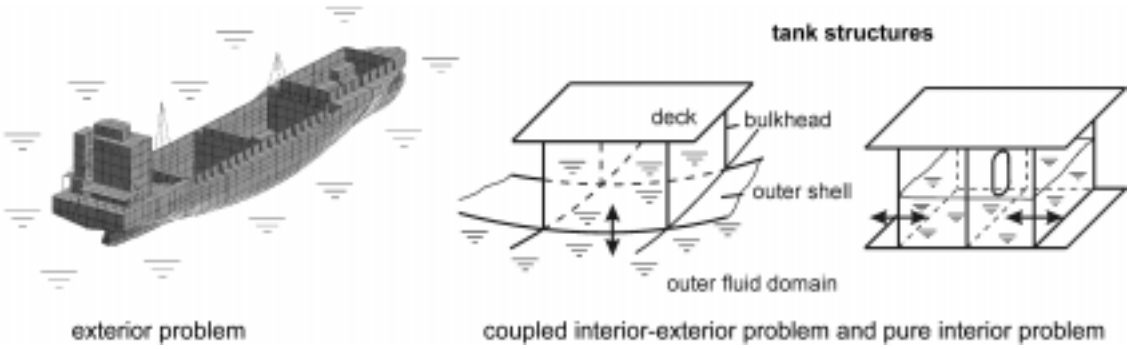

Fig. 1 Typical cases of application in vibration analysis

The fluid is mathematically modelled as potential-theoretical field problem when eliminating time variable according to the separation method:

$$\Delta\Phi = 0 \qquad \text{in } \Omega \text{ (fluid domain)} \tag{4a}$$

$$\Phi = 0 \qquad \text{on } \Gamma_1 \text{ (free water surface)} \tag{4b}$$

$$\frac{\partial\Phi}{\partial \boldsymbol{n}} = 0 \qquad \text{almost everywhere on } \Gamma_2 \text{ (canal bottom and canal walls)} \tag{4c}$$

$$\frac{\partial\Phi}{\partial \boldsymbol{n}} = h \qquad \text{almost everywhere on } \Gamma_c \text{ (contact surface)} \tag{4d}$$

$$\Gamma = \Gamma_1 \cup \Gamma_2 \cup \Gamma_c \tag{4e}$$

$$\Phi \in C(\overline{\Omega}) \qquad \text{with a regular normal derivative almost everywhere on } \Gamma \tag{4f}$$

$$\Phi = O(R^{-1}) \qquad \text{for} \quad R \to \infty \tag{4g}$$

Φ defines the velocity potential in the fluid domain Ω. Additionally to the cases shown in Fig. 1 problems with an outer fluid domain which is bounded in some directions are considered. The boundary condition on the free surface is (4b) (Dirichlet condition) when surface waves are excluded. The potential function Φ on the remaining boundary satisfies Neumann conditions. Those are homogeneous boundary conditions on solid walls (canal walls, bottom) and inhomogeneous on the contact surface (see Fig. 2). The function h is assumed to be piecewise continuous, the boundary itself is piecewise of class C^2 type. The usual requirements of differentiability on Φ are defined by (4f). In the case of an unbounded domain Ω the decay condition (4g) holds.

It is well-known that the problem (4) is uniquely solvable provided that the Dirichlet-boundary doesn't vanish in (4b). For numerical handling with BEM the direct method is used. Therefore (4) needs to be transformed into an integral equation:

$$\alpha(\boldsymbol{x})\Phi(\boldsymbol{x}) = V^0(\boldsymbol{x}, \partial\Phi, \Gamma_1) + V^0(\boldsymbol{x}, h, \Gamma_c) - V^1(\boldsymbol{x}, \Phi, \Gamma_2 \cup \Gamma_c) \qquad \forall \boldsymbol{x} \in \overline{\Omega} \tag{5a}$$

$$\Phi = 0 \qquad \text{on } \Gamma_1 \tag{5b}$$

$$\Phi \in C(\overline{\Omega}) \qquad \text{with a regular normal derivative almost everywhere on } \Gamma \tag{5c}$$

$$\Phi = O(R^{-1}) \qquad \text{for} \quad R \to \infty \tag{5d}$$

$$V^0(\boldsymbol{x}, \partial\Phi, \Gamma) = \int_\Gamma \frac{1}{|\boldsymbol{x}-\boldsymbol{y}|} \frac{\partial}{\partial \boldsymbol{n}_y} \Phi(\boldsymbol{y})\, d\Gamma_y \qquad \text{(single layer potential)}$$

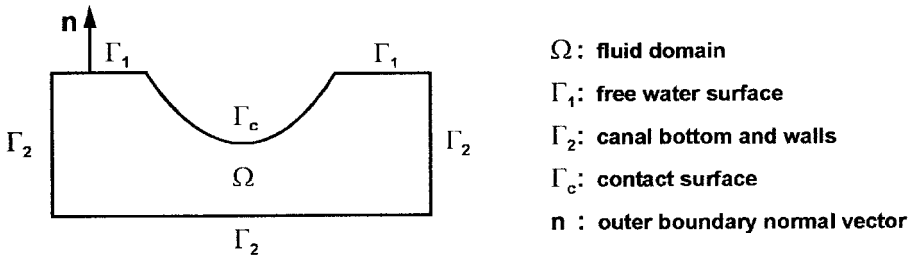

Fig. 2 Sectional view of the fluid domain

$$V^1(\boldsymbol{x},\Phi,\Gamma)=\int_\Gamma \Phi(\boldsymbol{y})\frac{\partial}{\partial \boldsymbol{n}_y}\frac{1}{|\boldsymbol{x}-\boldsymbol{y}|}d\Gamma_y \qquad \text{(double layer potential)}$$

(5a) has to be satisfied at every point $\boldsymbol{x}$ of Ω and its boundary. For deriving this matter of fact Green's identity is used inside the fluid domain. The validity on Γ follows from some limit relations (Brebbia, Telles and Wrobel 1984, Vladimirov 1977). Parameter $\alpha(\boldsymbol{x})$ is a function of geometry: Inside Ω it is 4π, outside $\overline{\Omega}$ it is 0, on Γ the value varies between both while for smooth segments 2π is assumed. It can be shown that the boundary value problem (4) and the integral equation problem (5) are equivalent and uniquely solvable.

3. The two-dimensional discrete model

The stepwise derivation of a BEM procedure is described in the following. It has to be kept in mind that the integral Eq. (5a) under continuity, differential and boundary conditions is still a three-dimensional problem. Also while discretization it needs a relation to the inner domain since the definition of an outer boundary normal derivative would be senseless otherwise. So the finally resulting boundary element formulation is a restriction of a makeshift three-dimensional discrete problem.

The function space W in which (5) is defined contains all functions being continuous in the fluid domain and on their boundary, having a regular boundary normal derivative almost everywhere on Γ and satisfying the Dirichlet conditions of the problem. (5) is uniquely solvable in this space. This allows a three-dimensional discretization: A mesh of octahedral elements according to Fig. 3 is assumed with tri-linear geometrical adaptation but globally continuous, element-wise tri-polynomial interpolation functions of uniform k^{th} degree ($k > 0$).

A collocation method with collocation points defined at the nodes is converging in the way of a h-refinement. The $(n+1)^{\text{th}}$ mesh should be generated by dividing all elements of the n^{th} mesh. This gives a progressive sequence of function spaces. Each refinement step adapts the outer mesh contour closer to the real geometry of Γ. It can be realised easily that the chosen interpolation functions are elements of W if the Dirichlet boundary condition is in addition required explicitly. All those elements having a common side-area with the boundary Γ are to be called first layer elements (refer to Fig. 3).

The resulting equation system contains in the horizontal row i the Eq. (5a) required at collocation point i. It couples the first m degrees of freedom (right hand side of 5a) with the i^{th} one (left hand

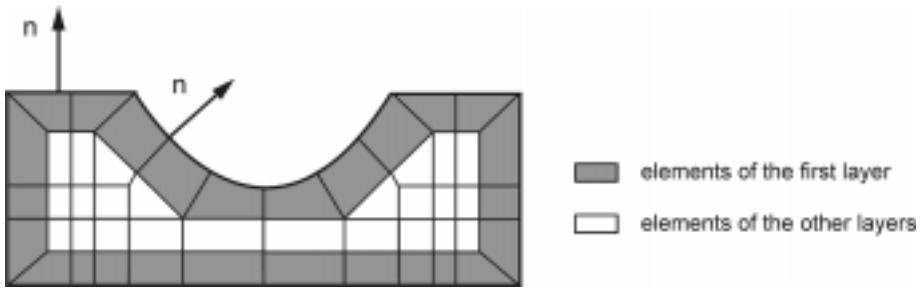

Fig. 3 Mesh of the makeshift 3D finite element model

side of 5a). That means the first m equations include only the first m degrees of freedom, those belonging to the first layer elements. This sub-system can be solved separately. Since the behaviour of Φ is of interest on Γ only the problem will be restricted to the equations of the first layer elements.

In the n^{th} discrete problem presented above a global discontinuous approximation of the continuous interpolation functions of the potential Φ and its normal derivative $(\partial\Phi/\partial\boldsymbol{n})$ by piecewise tri-polynomial functions in element-wise Cartesian co-ordinate systems of k^{th} degree in x and y as well as of first degree in z can be found in a way that the error of this approximation vanishes for $n \to \infty$. The so defined approximation functions don't satisfy Eq. (5a). But the residuum will vanish for $n \to \infty$ because the single layer and the double layer potential are continuous functions of $(\partial\Phi/\partial\boldsymbol{n})$ and Φ, respectively.

On the other hand it is an analogous deduction that global discontinuous and element-wise tri-polynomial shape functions satisfying (5a) in some suitable collocation points are approximating the analytical solution of the problem (5) in the n^{th} discrete problem with vanishing numerical error for $n \to \infty$. Restriction to the boundary Γ gives the equivalent and uniquely solvable two-dimensional problem (6) in two-field formulation with separate global discontinuous and element-wise bi-polynomial interpolation for Φ and $(\partial\Phi/\partial\boldsymbol{n})=\Psi$ formulated in local Cartesian co-ordinate systems. (The same functions are chosen for Φ and Ψ.) It can be shown that now even a polynomial degree of 0 is suitable in this two-field formulation (constant boundary elements).

All collocation points are placed on Γ in the interior of the boundary elements. It needs to be guaranteed that the collocation points are forming an "admissible system".

Remark: An element system should be designated as "admissible" if Haar's matrix (the value matrix of the interpolation functions at these points) is regular.

$$2\pi\Phi(\boldsymbol{x})=V^0(\boldsymbol{x},\partial\Phi,\Gamma)-V^1(\boldsymbol{x},\Phi,\Gamma) \qquad \text{for all collocation points } \boldsymbol{x}\in\Gamma \tag{6a}$$

$$\Phi=0 \qquad \text{on} \quad \Gamma_1 \tag{6b}$$

$$\Psi=0 \qquad \text{on} \quad \Gamma_2 \tag{6c}$$

$$\Psi=\hat{h} \qquad \text{on} \quad \Gamma_c \tag{6d}$$

$$\Phi=O(R^{-1}) \quad \text{for} \quad R\to\infty \tag{6e}$$

$\hat{h}$ is an element of the space of shape functions converging to h for $n \to \infty$.

The geometric factor $\alpha(x)$ is defined in (6a) as 2π since the inner-element collocation points have got a smooth (even plane) neighbourhood.

4. The element concept

Besides reducing the problem dimension and the effort (especially for the pre-processing) the BEM offers high flexibility when choosing suitable elements due to neglecting the continuity requirements on the functions. Complete families of elements can be developed systematically following simple procedures. Bi-polynomial functions in elemental x-y-co-ordinates of arbitrary order are to be defined using an appropriate number of collocation points without changing the mesh geometry as described above.

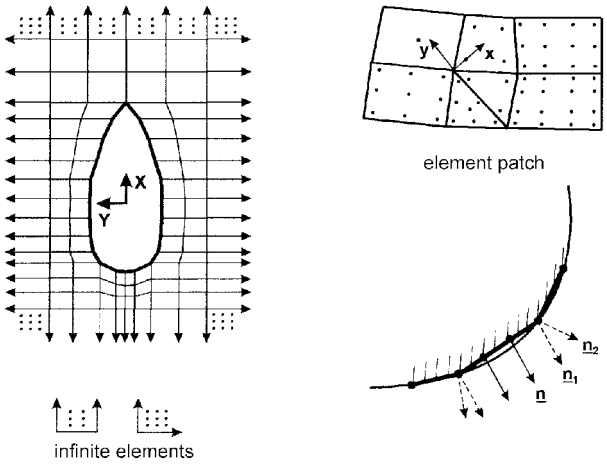

Fig. 4 Boundary element mesh of finite and infinite elements

Quadrilateral as well as triangular finite boundary elements are used. If Cartesian element coordinate systems are applied a fully analytical element-wise integration can be done in (6a) instead of the usual numerical integration.

In addition the transfer of the collocation points inside the elements solves the problem of non-unique boundary normal vectors in these points, see Fig. 4. The contact surface as well as the bottom and the canal walls (in case of bounded fluid domain) are modelled with finite boundary elements. Fig. 4 depicts a possible mesh on the free water surface. Starting from the structure the water surface is modelled with finite elements until a geometrically rectangular contour is reached. In case of unbounded fluid domain this contour is surrounded by infinite boundary elements allowing an effective description of such a surface: A single layer of these elements represents the entire remaining X-Y-plane.

A detailed description of the meshing technique with infinite boundary elements follows. Today a widely used method to model unbounded domains is to operate with a sufficiently wide limited area accepting an additional (even small) error. That leads to some problems in terms of implementation and deployment:

- The solution behaviour in the infinity is not reproduced exactly. For sufficiently wide “canal” dimensions this fact is practically without influence, because wall effects are negligibly small, but
- the effort for creating a mesh on the free water surface is increasing enormously for extremely large canal dimensions which causes a loss in efficiency of the program.
- The user therefore is forced to start with optimal parameters a priori which is hardly possible since they depend on the problem. To find a safe and reliable optimum (most slim canal without relevant wall effects) requires several complete calculation procedures, a method which is not acceptable.

An elegant solution of these problems is given by using infinite boundary elements. This terminus implies that geometrically unbounded areas can be modelled and the decay behaviour of the concerned field variable is simulated by suitable “semi-analytical” functions. Research related to this topic was running for years, some basically theoretical relationships are explained in (Bettes and

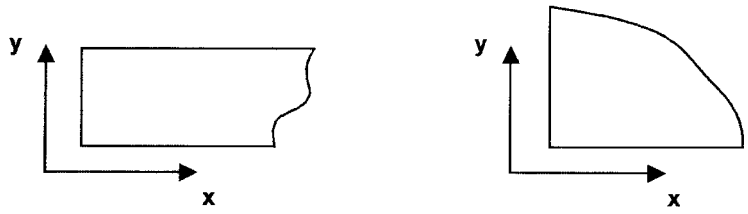

Fig. 5 Classification of infinite elements according to the geometry

Bettes 1979). The application of such elements mainly takes aim at increasing efficiency of the algorithm described here.

The rectangular element form is in general suitable for the presented case, offering the advantage of semi-analytical integration. That means an analytical calculation of the inner and a numerical calculation of the outer integrals in (6a) can be used. (A fully analytical integration is not practicable for infinite elements due to the complicated form of the integrand – weak singularity is possible – and unlimited domain of integration.) Fig. 5 displays the geometric classification of infinite elements according to the usage in Fig. 4. Both types have been implemented in a BE-program (Möller and Röhr 2000, Reich 1998).

The deployment of functions for the "infinite co-ordinate direction" to simulate the decay behaviour is a special feature of infinite elements. Inverse polynomials of the type

$$a_0+a_1 \cdot x^{-1}+\cdots+a_n \cdot x^{-n} \tag{7}$$

are used, the requirement a_0=0 guarantees the necessary $O(x^{-1})$-characteristic for the interpolation function. In addition a second type (8) of shape functions has been implemented in the BE-program.

$$(a_0+a_1 \cdot x^{1}+\cdots+a_n \cdot x^{n}) \cdot e^{-\frac{x}{L}} \tag{8}$$

The exponential decay behaviour of these functions is sufficiently fast in the "remote-field" in both cases, with the group of exponential decay functions much faster than required. Nevertheless both classes are proved to be as good as the other in practical examples. The possibility of semi-analytical integration however is given in the case of type (7) only.

In the case of infinite strip elements the same shape functions as for the finite boundary elements are used in the y-direction, refer to Fig. 5.

To estimate the position of the collocation points in global co-ordinates the transformation (9) is used for an equidistant distribution of the ξ_i in the interval (–1; 1).

$$x=\frac{1+\xi_i}{1-\xi_i} \cdot K+d \tag{9}$$

The maximum possible order of polynomials or inverse polynomials has been limited to 5 per co-ordinate direction in the BE-program (Reich 1998). Practical numerical convergence investigations (bi-linear interpolation functions for both the structure and the fluid model assumed) prove that the significant higher calculation effort of BEM (no sparse system matrix) is reflected in much more

accurate results. A series of test calculations with known analytical solution revealed that the separated relative error the BEM-program has contributed to the total error amounts to some percent only (for details refer to chapter 8). The errors from FE-calculation and from BE-calculation are of the same order of quality for constant BE-interpolation and bi-linear FE-interpolation. So the use of finite boundary elements with an order higher than 0 therefore is not efficient. In the following finite boundary elements and infinite strips in the "finite direction" are always considered with constant interpolation.

5. Calculation of the added mass matrix

The discretization of boundary integral Eq. (6a) gives a linear equation system (10) taking the boundary conditions (6b), (6c) into account.

$$\hat{\boldsymbol{H}} \cdot \varphi = \hat{\boldsymbol{G}} \cdot \psi \tag{10}$$

with the generalized parameter vectors φ and ψ. After elimination of variables being not of interest the resulting system is reduced to the degrees of freedom which are associated with the contact surface:

$$\boldsymbol{H} \cdot \varphi_c = \boldsymbol{G} \cdot \psi_c \tag{11}$$

The solution of this system and therefore of the whole fluid problem gives a linear dependence of the potential vector φ_c on the vector of its normal derivatives ψ_c, see (12). $\boldsymbol{C}$ is called "connectivity matrix".

$$\varphi_c = C \cdot \psi_c \tag{12}$$

The coupling between structure and fluid model is realised by the Neumann condition (4d) on the contact surface Γ_c with the normal velocity distribution of the structure h. In the case of being interest it is assumed as a globally continuous and element-wise bi-linear function on Γ_c according to the bi-linear FE-formulation of the structure. The chosen shape functions of the problem (6) do not satisfy this demand exactly. It is replaced by the approximate condition (6d) where the bi-polynomial function (in Cartesian element co-ordinates) $\hat{h}$ is given for each element Γ_m by

$$\int_{\Gamma_m} [\hat{h} - h]^2 d\Gamma \rightarrow \text{minimum} \tag{13}$$

(6d) and (13) lead to a coupling of fluid and structure model by the relation (14) between the parameter vector of the distribution of the boundary outer normal derivative of the fluid domain and the vector of structure node velocities.

$$\psi_c = \boldsymbol{R} \cdot \dot{\boldsymbol{D}} \tag{14}$$

Finally the potential vector depends on the degrees of freedom of the node displacements of structure. Based on an energetic principle the hydrodynamic added mass matrix is calculable by

$$\boldsymbol{M_H} = \frac{1}{2}(\hat{\boldsymbol{M}}_{\boldsymbol{H}} + \hat{\boldsymbol{M}}_{\boldsymbol{H}}^T); \quad \hat{\boldsymbol{M}}_{\boldsymbol{H}} = \boldsymbol{R}^T \cdot \boldsymbol{C}^T \cdot \boldsymbol{Q} \cdot \boldsymbol{R}; \quad \boldsymbol{Q} = \rho_f \int_{\Gamma_c} \boldsymbol{N}_c^T(y) \boldsymbol{N}_c(y) d\Gamma \tag{15}$$

where $\boldsymbol{N}_c$ denotes the vector of shape functions of the boundary elements on the contact surface and ρ_f the fluid density.

6. Non-connected fluid domain

The practical background to extend the program functionality to non-connected fluid domain is provided by the demand to deal with ship internal, partly or fully filled tank structures while considering the outer ship fluid field, refer to Fig. 1.

The basic problem in the mathematical formulation is the necessity to model two-dimensional structure elements wetted from both sides. The following geometry-specific definitions are agreed upon:

Def. 1: A subdivision of the entire fluid domain Ω into the n+1 sub-domains Ω_0 (outer area) and Ω_1, ... , Ω_n (inner sub-domains) is called cluster division of Ω if and only if

(a) every Ω_i is connected,
(b) the union of two different arbitrary subdomains $\Omega_i \cup \Omega_j$ is not connected,
(c) the boundary $\partial\Omega_i$ of an arbitrary subdomain is divided into two non-empty parts, a Dirichlet- and a Neumann-boundary corresponding to problem (4).

The subdomains Ω_i are named clusters.

Def. 2: A cluster Ω_i of a cluster division $\{\Omega_0, \Omega_1, \ldots, \Omega_n\}$ is named of the first kind if and only if there is no surface $S \subset \partial\Omega_i$ belonging to the boundary $\partial\Omega_i$ with both sides, upper and lower side. Otherwise Ω_i is named a cluster of the second kind. The whole domain Ω is a fluid domain of the first kind if it consists of clusters of the first kind only, otherwise it is named fluid domain of the second kind.

Remark: Def. 2 classifies clusters in accordance with the characteristics of partial boundary surfaces wetted on both sides: If there do not exist such a surface or if there exists a both side wetted surface but wetted by the fluid of two different clusters, so the considered cluster is of the first kind. Fig. 6 for instance shows a fluid domain of the first kind – it only contains clusters of the first kind.

Analogous to the so far handling of the outer fluid problem the algorithm described above is used for each separate domain Ω_0, ..., Ω_n. n+1 boundary value problems are defined and transformed into boundary integral equation problems. So there is no essential difference in handling fluid domains of the first kind compared with the procedure for only the exterior problem. The hydrodynamic

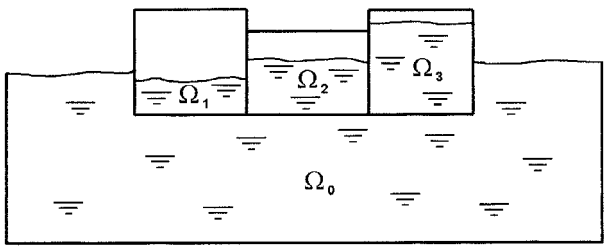

Fig. 6 Fluid domain of the first kind

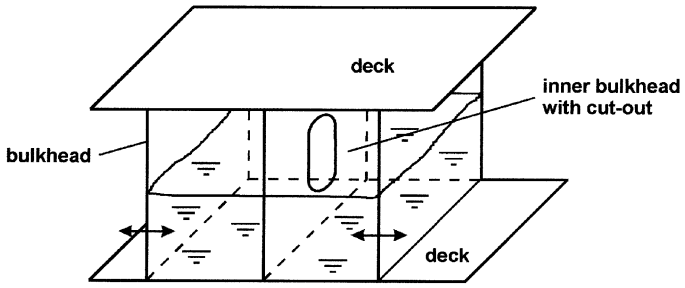

Fig. 7 Typical example of a cluster of the second kind

added mass matrices calculated for each sub-domain separately have to be added to form the total added mass matrix.

The problem of both side wetted elements, wetted by the fluid of different sub-domains is taken into account explicitly: The contact conditions required for the element's upper and lower side, respectively are combined directly by coupling them with the same normal velocity degree of freedom of the structure. This is a basic difference to a fluid domain of the second kind discussed now.

Fig. 7 depicts a typical example of a cluster of the second kind. The part of the inner bulkhead lying below the free surface of the fluid is wetted on both sides by the fluid of the very same cluster, because the two parts of the tank are connected by a cut-out of the bulkhead.

Remark: It has to be mentioned explicitly that the classification of def. 2 does not depend on the structure geometry only but also on the fluid level. For a sufficient low fluid level in the tank of Fig. 7 the fluid domain is of the first kind consisting of two clusters of the first kind.

For the structure model a two-dimensional idealisation of the plates is carried out. Both sides of such a plate element are part of the fluid boundary, need to be elements in the BE-program and have to be attached to collocation points, see Fig. 8.

The outer normal vectors are always pointing to the outside of the fluid domain as shown in the sketch of Fig. 9 with separated side areas.

This coupling of a single structure plate element with two potential boundary elements may cause theoretical inconsistencies between physical and mathematical model as well as enormous difficulties in the numerical realisation. The idea to assign both side areas of a structure plate element to boundary elements having the same geometry and identical collocation points failed as well as the approach taking a thickness d of the structure into account.

Only the transformation to a fluid domain of the first kind is a possible way. Fig. 10 depicts a

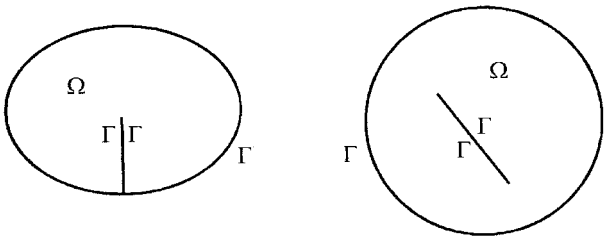

Fig. 8 Characteristic geometry of fluid domains of the second kind

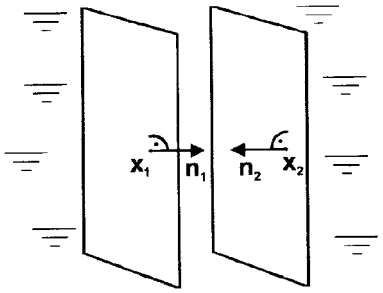

Fig. 9 Outer boundary normal vectors of a structure element wetted on both sides

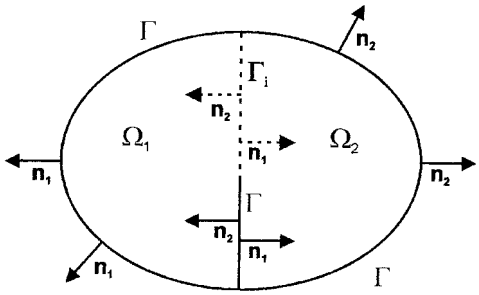

Fig. 10 Transformation of a fluid domain of the second kind by partitioning

principle sketch. The considered domain Ω is divided into two sub-domains (Ω_1 and Ω_2) by adding an internal boundary part Γ_i.

Theorem 1 is the basis for such a partitioning. This theorem investigates under which circumstances a piecewise harmonic function is harmonic in the entire domain. There is an analogue result for more than two sub-domains Ω_j.

Theorem 1: Under the geometrical assumptions fixed above (16) and (17) are equivalent:

u is a harmonic function in Ω. (16)

u_j are harmonic functions in Ω_j for $j \in \{1; 2\}$ and on Γ_i holds (17)

$$u_1 = u_2;\ \frac{\partial u_1}{\partial \boldsymbol{n}_1} = -\frac{\partial u_2}{\partial \boldsymbol{n}_2}$$

(with u_j as restriction of u onto the sub-domain Ω_j).

Proof: Assuming (16) in particular u is a harmonic function in the interior of the subdomains Ω_1 and Ω_2. Besides that u as harmonic function is in $C^{\infty}(\Omega)$ and therefore the continuity behaviour of u and its normal derivative on Γ_i holds, that means (17) is proofed.

Assume (17) now. Let $\varphi \in C_0^{\infty}(\Omega)$ be an arbitrary test function with compact support. So (18) holds because $\Delta u_j = 0$ in Ω_j.

$$\int_{\Omega_1} \varphi \Delta u_1 d\Omega + \int_{\Omega_2} \varphi \Delta u_2 d\Omega = 0 \tag{18}$$

φ and u_j are elements of $C^{\infty}(\Omega_j)$ and therefore satisfy the conditions of Green's theorem. It leads to

$$\int_{\Omega_1} u_1 \Delta \varphi d\Omega + \int_{\Omega_2} u_2 \Delta \varphi d\Omega + \int_{\Gamma_i} \left(\varphi \frac{\partial u_1}{\partial \boldsymbol{n}_1} - u_1 \frac{\partial \varphi}{\partial \boldsymbol{n}_1} + \varphi \frac{\partial u_2}{\partial \boldsymbol{n}_2} - u_2 \frac{\partial \varphi}{\partial \boldsymbol{n}_2} \right) d\Gamma = 0 \tag{19}$$

(All boundary integrals on Γ are vanishing cause of the compact support of φ.) φ and its derivatives are continuous on Γ_i. Taking the relations $\boldsymbol{n}_1 = -\boldsymbol{n}_2$; $u_1 = u_2$; $(\partial u_1/\partial \boldsymbol{n}_1) = -(\partial u_2/\partial \boldsymbol{n}_2)$ into account additionally the integral on Γ_i vanishes too in (19). So

$$\int_{\Omega_1} u_1 \Delta \varphi d\Omega + \int_{\Omega_2} u_2 \Delta \varphi d\Omega = \int_{\Omega} u \Delta \varphi d\Omega = 0 \tag{20}$$

is valid. (20) describes the weak Laplace equation. So because u is an element of $L_2(\Omega)$ it is a weakly harmonic function in Ω. Finally (16) follows from Weyl's lemma. concludes the proof of Theorem 1.

The numerical realisation corresponds to a sub-structure method. The elements of the additionally inserted boundary part Γ_i might be named virtual elements. The numerical treatment of a fluid domain of the second kind therefore is in accordance with the processing of a first kind domain under constraints.

7. Implementation

The entire algorithm of the hydroelastic vibration analysis is divided into three main parts.

1. Estimation of the hydrodynamic added mass matrix by the BEM-program HYDROEL.
2. Calculation of structure stiffness and structure mass matrix by FEM as well as adding up structure mass and hydrodynamic added mass matrix.
3. Solution of the general eigenvalue problem (3).

Points 2 and 3 have to be realised by commercial software components.

The BEM-program HYDROEL deals with an algorithm for calculation of the hydrodynamic added mass matrix as described above. In particular it is able to handle the exterior, the interior and the coupled exterior-interior problem. In the case of an outer fluid domain the cluster Ω_0 also may be bounded in some directions (shallow water or canal conditions). The program is coded in FORTRAN 90-standard.

It includes a pre-processor for automatic generating the BE mesh on the wetted surface of structure, the free surface of the fluid and the canal walls and bottom. For inner domains the meshing principle is quiet simple. After partitioning of clusters of the second kind as described in chapter 6 the fluid surface of every subdomain constructed by addition of virtual elements according to theorem 1 is meshed as shown in the sketch in Fig. 11.

For a bounded outer fluid domain the pre-processor creates a mesh as depicted in Fig. 12. For unbounded domains refer to Fig. 4.

The user may vary the position of the structure model to define some geometric parameters, the draught of a ship, for instance, the filling level of tanks or a nose-up vessel trim. The water line is

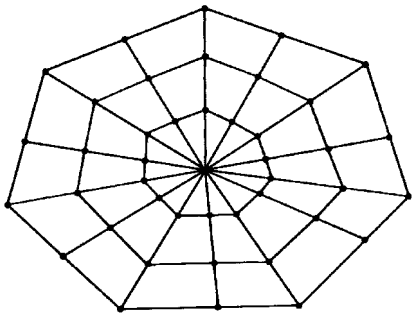

Fig. 11 Boundary element mesh of the free fluid surface for interior problems

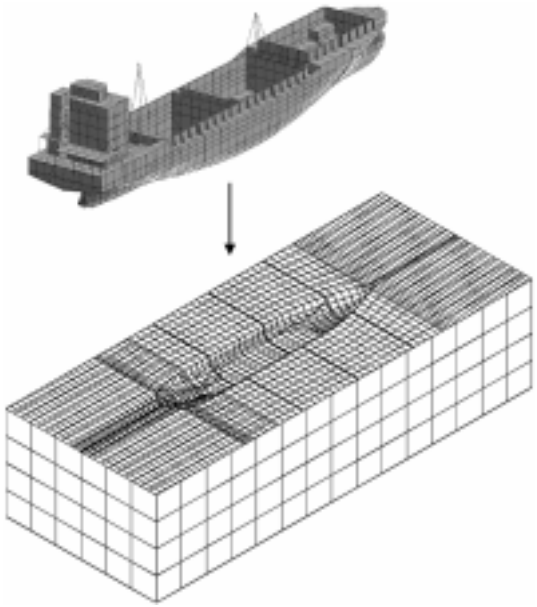

Fig. 12 Automatic mesh generation for a bounded fluid domain

defined as intersection between the structure model and the free fluid surface plane z=0. So the pre-processor in general has to generate new nodes and elements.

Collocation points are placed in the interior of the boundary elements in accordance with the order of the shape functions.

After calculation of all element integrals (see 6a – analytical calculation for finite boundary elements, half-analytical one for infinite elements with inverse polynomial shape functions, fully numerical calculation for infinite elements with exponential decay behaviour) being necessary to form the equation system (10) and reducing to the form (11) the solution of the equation system leads to the connectivity matrix and the final result is the added mass matrix (15) as described in chapter 5. This algorithm works cluster-wise, see chapter 6, and the resulting added mass matrix is formed by summation of all cluster matrices.

As all boundary solution processes involve very large full matrices, especially if applied in a fully three-dimensional case, as alternative solution method a mode superposition algorithm was implemented (Möller and Röhr 2000).

It shall be mentioned that the handling of the pure Neumann problem is not possible yet with the present programme version, but this does not contain theoretical difficulties.

8. Test calculations

A series of academic test examples has been modelled in order to verify the program as well as study convergence and efficiency. So the analytical solution for a single-side wetted square plate opposite to a solid wall is available, Fig. 13.

To deal with bi-linear shape functions for finite boundary elements a special test version of the program was coded. The main result of these investigations is the fact that bi-linear shape functions

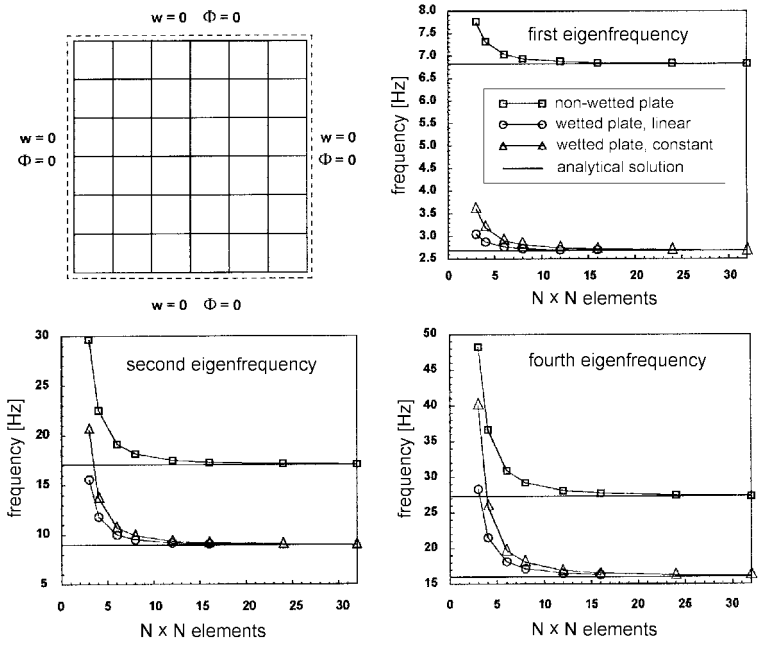

Fig. 13 Calculation example “one-side wetted plate opposite to a solid wall”

for the structure model and constant finite boundary elements are compatible with regard to numerical accuracy. The choice of shape functions of higher order for the finite boundary elements however leads to a rapidly increasing numerical effort not justified by the achieved relatively little decreasing numerical error of the entire problem (because of the superposition of the numerical errors of the FE and the BE-calculation).

A practically relevant model shall be discussed now, a container vessel, refer to Fig. 1, left hand side. The results from eigenfrequency analysis contain beside a comparison with the method of added masses by Lewis (see Fig. 14) the verification that the calculation model presented here is applicable to special fairway conditions.

For the investigations on the influence of fairway depth the advantages of three-dimensional mass modelling emerge clearer. So the eigenvibration behaviour of the vessel as a function of water depth is considered, refer to Fig. 15. The frequency spectrums including those for deep water are summarized. As expected frequencies decline with decreasing water depth (h/D) for a fixed mode of vibration.

Focussing on the frequency changes only no conclusion can be obtained with regard to the real hydrodynamic influence on the structure. While considering the transition from deep water (h/D =7.5) to canal conditions of h/D=1.6 for the 12^{th} mode only a slight frequency decline of 2.4 per cent is detectable. It is raising only for extreme decreased water depth (h/D=1.2) up to 9 per cent. Taking the assigned modes of vibration, the deformation modes of same order, into consideration the hydrodynamic influence becomes more clear. Even frequency changes of this quantity lead to transition into another mode.

Looking at the very same mode, e.g. the deck house mode (refer to Fig. 16), in the frequency spectrums calculated for different water depth an interesting observation can be done. Whereas the mode by itself remains almost unaffected the related frequency varies by more then 1 Hz. This

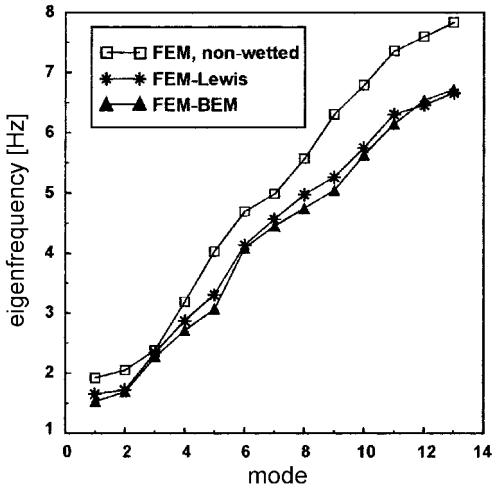

Fig. 14 Comparison of natural frequencies of a container vessel floating on water

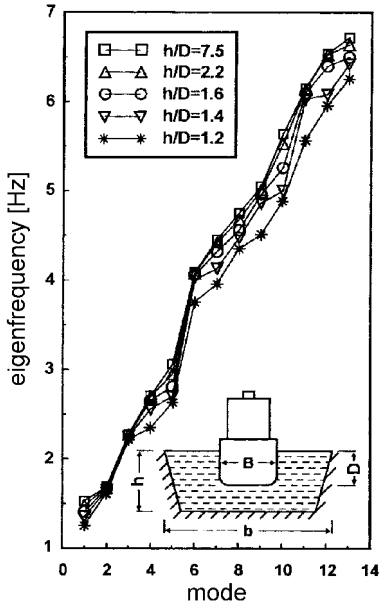

Fig. 15 Effect of water depth on natural frequencies of a container vessel floating on water

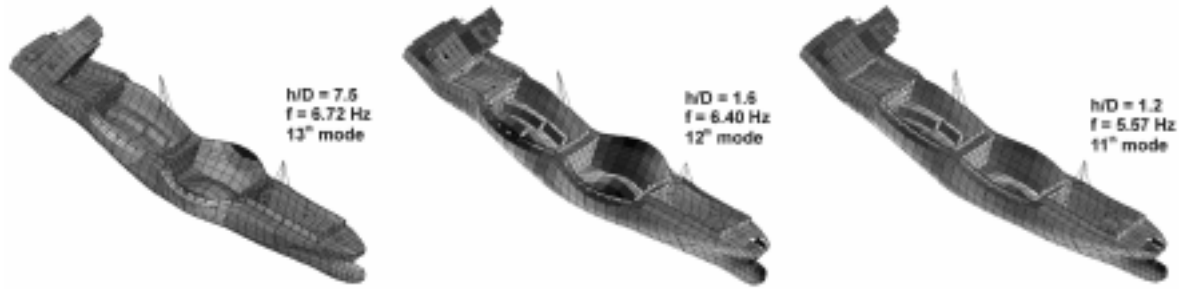

Fig. 16 Vibration modes of the deck house as function of water depth

"shifting-effect" of deformation modes might be of interest from a practical point of view.

Furthermore investigations have been carried out on the influence of vessel trim (nose-up trim) in eigenvalue analysis as well as on the problem of forced vibration.

The following test example for the interior problem focuses on a comparison of numerical and analytical solution again. Considered for this purpose are geometrical models of cubic, open-top, fully filled tanks with a partition bulkhead of variable height, Fig. 17. Each side wall has been modelled by a mesh of $2N \cdot 2N$ boundary elements.

A special test version of the program HYDROEL enables a direct comparison of calculated velocity potential values Φ with the analytical solution as a function of N. Some boundary conditions have been defined in a way that simple bi-linear solution functions are obtained. Two examples have been considered:

$$\Phi = z \text{ and } \Phi = z(4+3x+2y+xy) \tag{21}$$

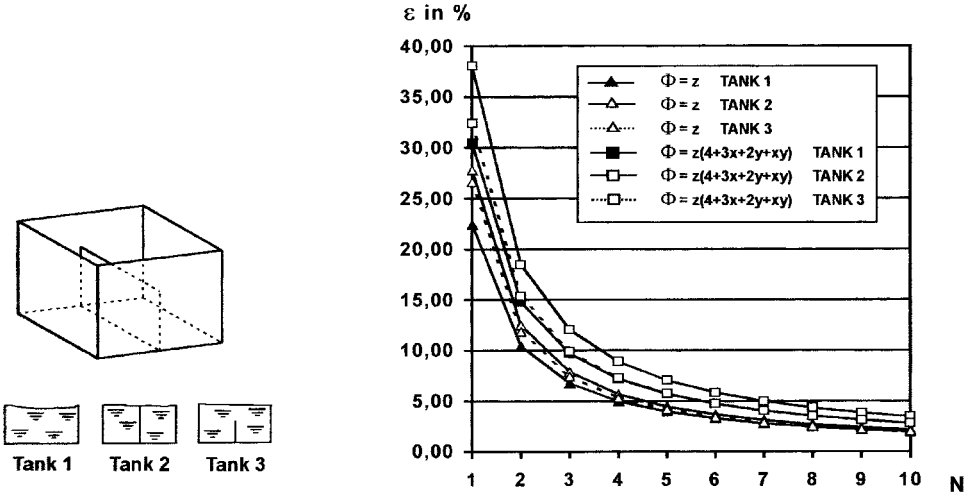

Fig. 17 Error estimation in the calculation example “filled tank”

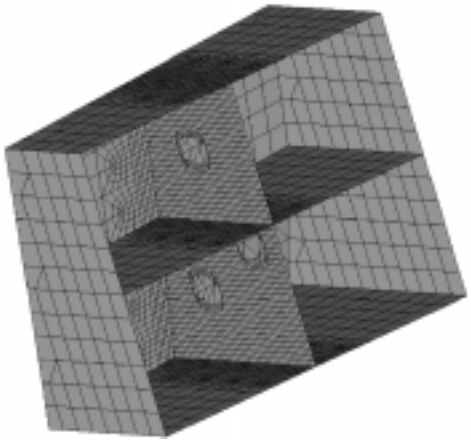

Fig. 18 Finite element model of the tank structure

The resulting relative errors based on the L_2-norm are depicted in Fig. 17.

Finally a practically relevant model has been investigated. Fig. 18 shows the finite element mesh of a tank taken from Jefferies (1998). The fluid attached to the nearly fully filled tank is a domain of the second kind because the filling level reaches the cut-outs in the bulkheads.

Table 1 shows the first eigenfrequencies. Fig. 19 presents some eigenmodes of special practical interest.

10. Conclusions

The paper has Presented an improved FE-BE-methodology to deal with hydroelastic vibration problems of complex thin-walled structures in maritime areas especially. The main aspects of the

Table 1 Natural frequencies of the tank structure

mode number	1	2	3	4	5	6	7	8	9	10	11
f in Hz	4.48	6.29	7.15	9.20	9.98	10.37	10.81	11.69	12.63	12.83	13.19
mode number	12	13	14	15	16	17	18	19	20	21	22
f in Hz	14.20	14.59	14.87	15.02	15.33	15.47	16.12	16.56	17.25	17.46	17.78
mode number	23	24	25	26	27	28	29	30	31	32	33
f in Hz	18.01	18.78	18.90	19.32	19.80	19.87	20.04	20.40	20.59	21.07	21.19
mode number	34	35	36	37	38	39	40	41	42	43	44
f in Hz	21.50	21.85	22.36	22.56	22.60	23.05	23.42	23.87	23.98	24.09	24.16

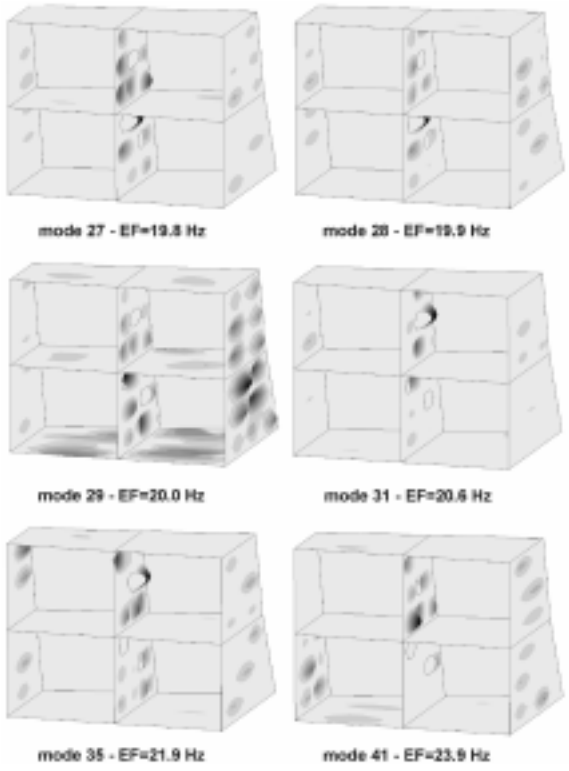

Fig. 19 Selection of eigenmodes of the filled tank structure considered

analysis have been derived in general terms and verified by studies related to numerical convergence as well as to practical applications. In details it could be shown that the proposed boundary element concept is able to meet theoretical and practical demands as

- Pre-processing by high-grade computer aided discretization of bounded and unbounded 3D as well as interior and exterior fluid domains.
- FE compatible and variable order concept of finite fluid boundary elements.
- Improved efficiency by infinite formulations for discretization of free surfaces of unbounded fluid domains.
- Numerical robustness of BE formulation for general fluid (thin-walled) structure configurations.

· Compatibility of BE fluid models to FE structural tools.

Acknowledgements

The authors are grateful to the Ministry of Education and Research of the Federal Republic of Germany for financial support.

References

Armand, J.-L. and Orsero, P. (1979), "A method for evaluating the hydrodynamic added mass in ship hull vibrations", *Transactions of SNAME* 87, 99-120.

Brebbia, C.A., Telles, J.C.F. and Wrobel, L.C. (1984), "Boundary element techniques", *Theory and Applications in Engineering*, Berlin, Heidelberg, New York, Tokyo, Springer.

Bettes, P. and Bettes, J.A. (1984), "Infinite elements for static problems", *Eng. Comput.*, **1**, March, 4-16.

Camisetti, C. *et al*. (1979), "Investigation of the containership vibration behaviour by finite element method at design stage", *Int. Conf. on Eng. Application of the Finite Element Method*, Høvik, Norway, May 9-11, 3.1-3.30.

Geßner, W., Schmitz, K.-P., Ahrens, J. and Herzberg, L. (1983), "Three-dimensional finite element models for calculation of global ship vibrations", Schiffbauforschung 22, 4, 205-213.

Hakala, M.K. (1986), "Application of the finite element method to fluid-structure interaction in ship vibration", Espoo September, Research Reports 433, Technical Research Centre of Finland.

Jefferies, H. (1998), "Fatigue strength of a bulb profile cut-out subject to propeller excitation", Diploma Thesis, Hamburg.

Landweber, L. (1957), "Added mass of lewis forms oscillating in a free surface", *Proc. Symposium on the Behaviour of Ships in a Seaway*, Wageningen, the Netherlands.

Lewis, F.M. (1929), "The inertia of the water surrounding a vibrating ship", *SNAME*, **37**.

Möller, P. and Röhr, U. (2000), "Hydrodynamic mass and damping matrices", Research Report of the Project "Life Cycle Design" (BMBF), University of Rostock.

Payer, H.G. (1981), "The influence of vibrations on the strength of ships", *Jahrbuch der Schiffbautechnischen Gesellschaft*, Berlin, Heidelberg, New York, Springer, **75**, 290-294.

Payer, H.G. and Asmussen, I. (1985), "Vibration response on propulsion-efficient container vessels", *SNAME Transactions*, **93**, 147-164.

Payer, H.G. and Pleß, E. (1985), "Design and dimensioning of open type vessels with long hatches", *Jahrbuch der Schiffbautechnischen Gesellschaft*, Berlin, Heidelberg, New York. Springer, **79**, 323-326.

Reich M. (1998), "Development of infinite elements with semi-analytical integration for application in direct boundary element method", Diploma Thesis, University of Rostock.

Skaar, K.T. and Carlsen, C.A. (1979), "Modelling aspects for finite element analysis of ship vibration", *Int. Conf. on Engineering Application of the Finite Element Method*, Hovik, Norway, May 9-11, 4.1-4.30.

Vladimirov, V.S. (1977), *Equations of Mathematical Physics*, Berlin, Verlag der Wissenschaften.